

Ground-R1: Incentivizing Grounded Visual Reasoning via Reinforcement Learning

Meng Cao^{1*}, Haoze Zhao^{1*}, Can Zhang², Xiaojun Chang^{1,4},
Ian Reid¹, Xiaodan Liang^{1,3†}

¹MBZUAI ²Peking University ³Sun Yat-sen University
⁴University of Science and Technology of China

*Authors contributed equally to this research. †Corresponding author.

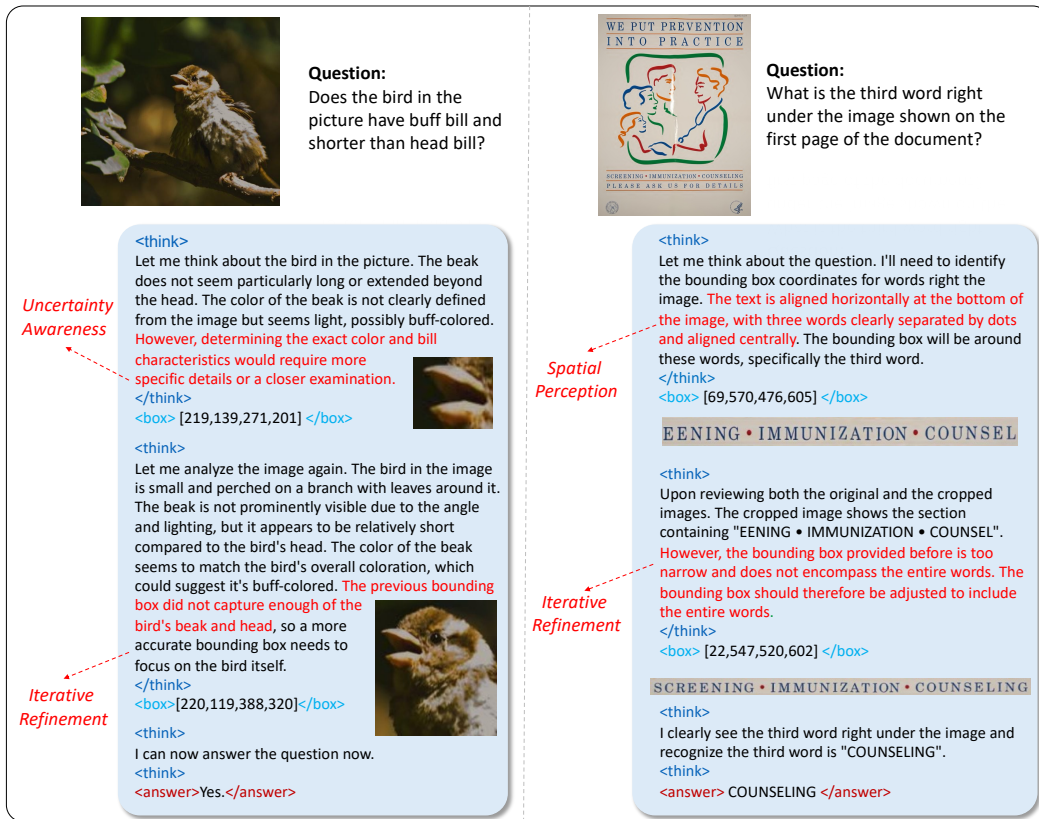


Figure 1: **Reasoning trajectories of Ground-R1.** Our method enables visual reasoning through automatic *zoom-in* operations while eliminating the need for explicit bounding box supervision, rationale annotations, or external tool calls. Ground-R1 exhibits human-like cognitive capabilities including uncertainty awareness, spatial perception, and iterative refinement. Refer to Appendix B for more visualization cases.

Abstract

Large Vision-Language Models (LVLMs) have demonstrated impressive general capabilities across a wide range of multi-modal tasks. However, the reasoning processes of LVLMs often suffer from unreliable outputs and limited interpretability. To address this, *grounded visual reasoning* has emerged as a promising paradigm

that enforces responses anchored on salient visual evidence regions. However, existing approaches typically rely on costly supervision such as bounding box annotations, chain-of-thought rationale or external tool calls, limiting their scalability. In this work, we propose Ground-R1, a reinforcement learning framework that enables grounded visual reasoning *without requiring explicit evidence or rationale annotations*. Ground-R1 consists of a grounding phase that generates evidence region rollouts based on format constraints, and an answering phase that produces responses guided by both answer correctness and format adherence rewards. Extensive experiments across multiple visual reasoning benchmarks manifest that Ground-R1 achieves superior performance and exhibits emergent cognitive behaviors such as uncertainty awareness, spatial perception, and iterative refinement, offering a scalable and interpretable alternative to existing approaches.

1 Introduction

Large Vision-Language Models (LVLMs) [38, 1, 3] have emerged as versatile general-purpose assistants, capable of interpreting and executing a wide range of real-world tasks through the unified processing of visual and linguistic signals. Despite their impressive capabilities, LVLMs still suffer from limited answer reliability and poor interpretability. These issues often stem from the models’ tendency to rely on spurious correlations in pre-training data distributions, rather than grounding their predictions in salient visual evidence from the input [13, 65, 75].

To mitigate these limitations, recent studies advocates *grounded visual grounding* [44, 42, 50, 61, 23, 40, 71], *i.e.*, a paradigm that requires models to explicitly anchor reasoning processes to *evidence regions* (*i.e.*, salient image areas supporting inferences) during chain-of-thought (CoT) analysis. As illustrated in Figure 1 (left), accurate question answering requires the model to initially ground the regions containing the bird’s beak and head in the image, followed by zoom-in operations on these localized areas for precise inference. Through this process, grounded visual reasoning enforces tight coupling between visual evidence and textual responses, yielding more reliable and interpretable outputs compared to conventional methods. However, existing grounded visual reasoning methods typically depend on costly human annotations such as bounding boxes [44, 42], CoT rationales [44] or external tool calls [48, 14, 32, 11] to supervise evidence region localization. For instance, Visual CoT [44] contains 438k annotated examples with intermediate bounding box supervision, which imposes significant resource burdens and limits scalability. Recently, R1-series studies [12, 66, 39, 51, 29, 36, 69] have been introduced to optimize policy models via online-generated *rollout* data, which demonstrates complex reasoning capabilities including self-correction and backtracking.

Motivated by these advances, we introduce Ground-R1, a reinforcement learning (RL) framework that enables grounded visual reasoning without requiring any bounding box supervision, rationale annotations or external tool calls. Specifically, Ground-R1 firstly analyzes input instructions and generates evidence region rollouts, which is solely supervised by the format constraints; Then it synthesizes response rollouts based on the input image, contextual reasoning traces, and zoom-in evidence regions, which is driven by both the format and accuracy maximization rewards. Ground-R1 enables end-to-end training that jointly optimizes evidence localization and response generation purely through question-answering supervision.

We evaluate Ground-R1 on a comprehensive suite of benchmarks spanning visual question answering, visual grounding, and hallucination detection. Our method consistently delivers strong performance over supervised fine-tuning (SFT) counterparts, grounded visual reasoning approaches [30, 44, 42, 30], and concurrent R1-series works [66, 39, 16]. For example, built upon Qwen2.5-VL [3], Ground-R1 achieves a 9.2% absolute improvement on VisCoTBench [44]. In addition, Ground-R1 demonstrates emergent cognitive behaviors such as uncertainty awareness, spatial perception, and iterative refinement, which replicates core attributes of human-like cognition. For example in Figure 1 (left), our Ground-R1 recognizes that the original image lacks specific details for reliable inference (*i.e.*, uncertainty awareness), and identifies inaccuracies in the previously generated evidence region during reasoning, prompting a re-generation (*i.e.*, iterative refinement).

In summary, our contributions are in three-folds:

- We propose Ground-R1, a novel RL framework for grounded visual reasoning that eliminates the need for costly bounding box annotations, CoT rationales, and external tool calls.
- Ground-R1 decouples evidence region generation from answer synthesis, enabling interpretable reasoning via format-constrained grounding and reward-driven response generation.
- Extensive experiments across multiple benchmarks demonstrate that Ground-R1 achieves superior performance and exhibits emergent cognitive behaviors such as uncertainty awareness, spatial perception and iterative refinement.

2 Related Work

Visual Reasoning in LVLMs. Recent advances in LVLMs’ visual reasoning capabilities have driven sustained research efforts toward implementing cognitive processes through explicit problem-solving trajectories [58, 15, 63]. The early attempts [8, 68, 4, 59] employ carefully designed prompts to guide the rationale generation. Tree-of-Thought [68] and Graph-of-Thought [4] overcome CoT’s single-path reasoning constraints by structuring multi-branch exploration through tree/graph topologies, enabling complex task-solving via divergent pathway analysis. Another kind of method enhances the reasoning capability of LVLMs through conducting SFT based on CoT rationale annotations [74, 55, 9, 64, 52, 67]. LLaVA-CoT [64] explicitly defines the structured reasoning stages to enhance the process interpretability. To take one step further, LlamaV-o1 [52] introduces a curriculum learning approach to facilitate incremental skill acquisition. Mulberry [67] augments Monte Carlo Tree Search by integrating collective knowledge from multiple LVLMs, where negative exploration paths are leveraged to synthesize self-reflective data for iterative self-correction.

However, such approaches not only necessitate CoT annotations but also demonstrate limited generalization capabilities [31]. Recent breakthroughs from DeepSeek-R1 [12] demonstrate that pure reinforcement learning can stimulate active reasoning processes in LLMs, encompassing self-reflection and self-correction. This discovery has catalyzed a wave of R1-inspired methodologies in vision-language research [66, 39, 51, 29, 36, 69, 16]. Vision-R1 [16] introduces a progressive thinking suppression training strategy to address overthinking issues. LMM-R1 [39] focuses on unleashing general reasoning capabilities in 3B-parameter models, demonstrating progress in visual geometry and agent domains. Visual-RFT [29] further extends this paradigm to broader vision tasks, including fine-grained classification and object detection. However, most existing methods process images only at the input stage while conducting reasoning exclusively through text. Our proposed Ground-R1 incorporates images into its reasoning chains, enabling dynamic visual operations such as zooming and cropping, which aligns with human cognitive patterns involving iterative visual interactions during reasoning processes.

Grounded Visual Reasoning. Recent grounded visual reasoning works [44, 42, 50, 61, 23, 40, 30, 9] propose to selectively identify crucial regions to facilitate interpretable reasoning, especially in complex and visually crowded scenarios. To achieve fine-grained region-level understanding, early works like GPT4RoI [72] are introduced to convert user-specified bounding boxes into region features. Kosmos-2 [40] grounds LVLMs to visual worlds by constructing large-scale grounded image-text pairs. V* [60] introduces a visual search process leveraging commonsense knowledge and contextual cues for detailed visual queries. While alternative approaches employ agent-based architectures for tool-assisted task execution [27, 23, 40, 71], they incur non-trivial computational overhead and remain fundamentally constrained by the capability ceilings of their external toolkits. Recent advancements, such as VisCoT [44], Vocot [23], CogCoM [42] and FAST [50], integrate representations of evidence regions into CoT processes, enabling interleaved multi-step reasoning. While these grounding-enhanced methods demonstrate impressive performance and improved interpretability, they universally rely on annotated evidence regions. In contrast, our proposed Ground-R1 employs reinforcement learning to stimulate cognitive behaviors including uncertainty awareness, spatial perception, and iterative refinement, achieving accurate evidence region localization and final predictions without requiring bounding box annotations.

3 Ground-R1

Our proposed Ground-R1 comprises the grounding phase for evidence region generation (Section 3.1) and the answering phase for response synthesis (Section 3.2). Each section details the rollout mecha-

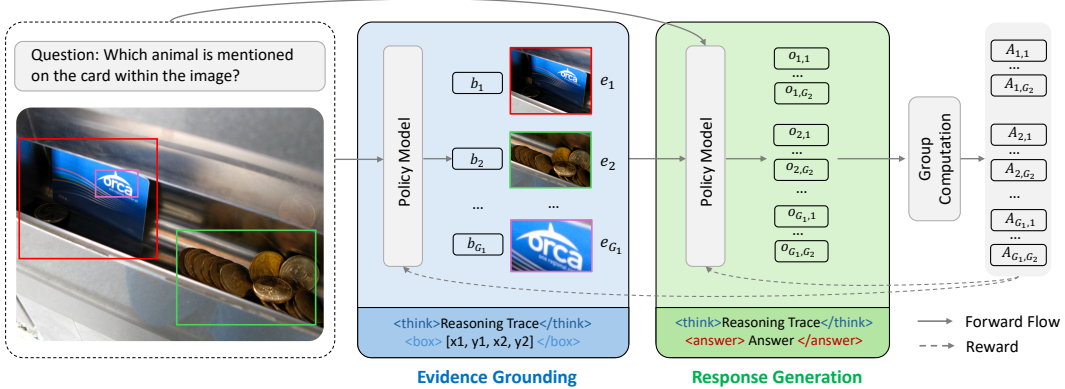


Figure 2: **Schematic illustrations of Ground-R1.** The **grounding phase** analyzes input instructions and generates evidence region rollouts, which are supervised by the format reward. $\mathbf{b}_i \in \mathbb{R}^4$ denotes the axis-aligned bounding box coordinates and e_i is the corresponding cropped evidence region, $i \in [1, G_1]$. **The answering phase** takes the input image, question, and the generated evidence regions as input and delivers final answers. This procedure is driven by both the format and accuracy maximization rewards. $o_{i,j}$ denote the j -th rollout answers based on the i -th evidence region e_i , $j \in [1, G_2]$. $A_{i,j}$ is the computed advantages (c.f. Eq. (4)).

nisms and reward formulation. Section 3.3 delineates the RL-based training process. The schematic illustrations and prompts of Ground-R1 are demonstrated in Figure 2 and Table 1, respectively.

Table 1: **Prompts for Ground-R1.** `{input}` will be replaced with the specific question and image during training and inference.

<p>Question: <code>{input}</code></p> <p>Please think about this question as if you were a human pondering deeply. Provide detailed reasoning between the <code><think></code> and <code></think></code> tags. Reason whether there exists a region in the image that could help you answer the question better. If such a region exists, provide one bounding box coordinate in the format <code>[x1,y1,x2,y2]</code> inside the <code><box></code> and <code></box></code> tags.</p> <p>Then, you will receive a cropped image based on the bounding box. Use all the images to continue reasoning. You may conduct multiple rounds of grounding to refine your region as you want. The bounding box you provide should always be selected based on the original image. If at any point you determine no further visual information is needed, you may directly provide the final answer inside the <code><answer></code> and <code></answer></code> tags.</p> <p>Format Example:</p> <p><code><think></code> Reasoning Process <code></think></code> <code><box></code> <code>[x1,y1,x2,y2]</code> <code></box></code> or, <code><think></code> Reasoning Process <code></think></code><code><answer></code> Final Answer <code></answer></code></p>
--

3.1 Grounding Rollout

Grounding Rollout Process. Given the input question q and image v , the grounding rollout process synthesizes critical evidence regions through iterative reasoning. We formally structure cognitive processes through dedicated markup tags: analytical reasoning flows are encapsulated within `<think>` and `</think>` elements, while visual grounding outputs are delimited by `<box>` and `</box>` tags.

Following GRPO [45], a set of grounding rollouts is generated by an existing policy $\pi_{\theta_{\text{old}}}$ as follows.

$$\mathbf{b} = \{\mathbf{b}_i\}_{i=1}^{G_1} \sim \pi_{\theta_{\text{old}}}(\cdot | \mathbf{q}, \mathbf{v}), \quad (1)$$

where $\mathbf{b}_i \in \mathbb{R}^4$ denotes the axis-aligned bounding box represented by its top-left and bottom-right corner coordinates. G_1 is the number of sampled grounding rollouts.

Reward Design. To mitigate annotation dependency on evidence regions, we merely constrain the grounding rollout process through structured format rewards rather than coordinate-level supervision. This is implemented by enforcing that the reasoning traces are bracketed within `<think>` and

`</think>` tags while corresponding spatial coordinates are structured within `<box>` and `</box>` tags. We denote the reward for the i -th rollout sample as r_i^{ground} , $i \in [1, G_1]$.

3.2 Answer Rollout

Answer Rollout Process. Leveraging the evidence region coordinates generated from the grounding rollout process, we extract corresponding image regions through spatial cropping. During the answer rollout phase, the policy model integrates multiple inputs including the original image, textual query, and evidence-aligned image regions to synthesize final responses. Consider a generated bounding box b_i as an illustrative case, the corresponding evidence region e_i is derived through zoom-in and cropping operations. The answer rollout process is formally expressed as:

$$\mathbf{o}_i = \{\mathbf{o}_{i,j}\}_{j=1}^{G_2} \sim \pi_{\theta_{\text{old}}}(\cdot | \mathbf{q}, \mathbf{v}, e_i), \quad i \in [1, G_1], \quad (2)$$

where $\mathbf{o}_{i,j}$ denote the j -th rollout answers based on the i -th evidence region e_i . G_2 denotes the number of answer rollouts generated per evidence region, yielding a total of $G_1 \cdot G_2$ reasoning trajectories in the two-phase procedures.

Reward Design. The answer rollout process integrates two complementary reward mechanisms:

- *Format rewards* ensures coherence by structuring reasoning traces within `<think>` and `</think>` tags and final answers within `<answer>` and `</answer>` tags.
- *Accuracy rewards* adapts to the question type, *i.e.*, the rewards for multiple-choice questions are binary based on exact answer matches while the reward for free-form questions is defined as the lexical alignment using the average of ROUGE-1, ROUGE-2, and ROUGE-L scores against ground-truth answers.

Formally, the overall reward for the j -th answer rollout conditioned on the i -th evidence region e_i is denoted as $r_{i,j}^{\text{answer}}$, $i \in [1, G_1]$, $j \in [1, G_2]$.

3.3 Reinforcement Learning Training

Our Ground-R1 is trained via the GRPO [45] framework that simultaneously coordinates evidence grounding and answer generation through reinforcement learning. The current policy is then optimized by maximizing the following objective function:

$$\mathcal{J}_{GRPO}(\theta) = \mathbb{E} \left[\mathbf{q}, \mathbf{v}, \{\mathbf{o}_i\}_{i=1, j=1}^{G_1, G_2} \sim \pi_{\theta_{\text{old}}}(\mathbf{o} | \mathbf{q}, \mathbf{v}) \right] \\ \frac{1}{G_1 \cdot G_2} \sum_{i=1}^{G_1} \sum_{j=1}^{G_2} \min \left(\frac{\pi_{\theta}(\mathbf{o}_{i,j} | \mathbf{q}, \mathbf{v})}{\pi_{\theta_{\text{old}}}(\mathbf{o}_{i,j} | \mathbf{q}, \mathbf{v})} A_{i,j}, \text{clip} \left(\frac{\pi_{\theta}(\mathbf{o}_{i,j} | \mathbf{q}, \mathbf{v})}{\pi_{\theta_{\text{old}}}(\mathbf{o}_{i,j} | \mathbf{q}, \mathbf{v})}, 1 - \varepsilon, 1 + \varepsilon \right) A_{i,j} \right), \quad (3)$$

where π_{θ} denotes the current policy model. $\mathbf{o}_{i,j}$ denote the j -th rollout answers based on the i -th evidence region (*c.f.* Eq (2)). ε are hyper-parameters. $A_{i,j}$ are the advantages computed using the group reward $\{r_{i,j}^{\text{answer}} | 1 \leq i \leq G_1, 1 \leq j \leq G_2\}$ as follows.

$$A_{i,j} = \frac{r_{i,j}^{\text{answer}} - \text{mean}(\{r_{i,j}^{\text{answer}}\}_{i=1, j=1}^{G_1, G_2})}{\text{std}(\{r_{i,j}^{\text{answer}}\}_{i=1, j=1}^{G_1, G_2})}. \quad (4)$$

4 Experiments

4.1 Experiment Settings

Dataset and Benchmarks. For training, we adopt the VisCoT dataset [44], which contains 438K visual question-answer pairs with bounding box annotations highlighting key image regions. To establish annotation efficiency, we employ a subsampled 1/50 fraction (8K samples) of the original data and deliberately discard bounding box annotations. For systematic evaluation, we benchmark Ground-R1 across a suite of benchmarks across visual question answering (VQA) and visual grounding:

- **Visual Question Answering:** The evaluated benchmarks include the test split of VisCoT [44], MME [10], MM-Vet [70], SEED-Bench [21], MME-RealWorld-Lite (MME-RWL) [73], Real-worldQA [62] and POPE [22], covering capabilities in document OCR, fine-grained understanding, chart reasoning, *etc.*

Table 2: **Evaluation results on the test split of VisCoT benchmark** including doc/text and chart understanding and general VQA, relation reasoning, and fine-grained VQA (FGVQA).

Method	AVG	Doc/Text					Chart
		DocVQA	TextCaps	TextVQA	DUDE	SROIE	InfoVQA
LLaVA-1.5-7B [CVPR24][26]	45.4	24.4	59.7	58.8	29.0	13.6	40.0
LLaVA-1.5-13B [CVPR24][26]	47.8	26.8	61.5	61.7	28.7	16.4	42.6
SPHINX-13B [arXiv23][24]	41.9	19.8	55.1	53.2	0.0	7.1	35.2
VisCoT-7B [NeurIPS24][44]	58.0	47.6	67.5	77.5	38.6	47.0	32.4
CogCoM [ICLR25][42]	–	–	–	71.1	–	–	–
Chain of Spot [arXiv24][30]	–	–	–	60.9	–	–	–
FAST [ICLR25][49]	–	–	–	60.7	–	–	–
Vision-R1-7B [arXiv25][16]	73.1	86.0	71.9	88.3	67.0	89.9	61.3
LMM-R1 [arXiv25][39]	69.2	84.3	78.0	91.2	66.7	78.5	55.6
R1-Onevision [arXiv25][66]	73.5	81.0	75.0	86.3	67.7	83.7	56.7
Qwen2.5-VL-7B [arXiv25][3]	72.5	88.0	81.5	88.4	72.3	88.7	67.1
Ground-R1 (Ours)	81.7	88.4	83.8	95.3	70.6	89.7	69.3
Δ (vs. Qwen2.5-VL-7B)	+9.2	+0.4	+2.3	+6.9	-1.7	+1.0	+2.2

(a)

Method	AVG	General VQA		Relation Reasoning			FGVQA
		Flickr30k	Visual7W	GQA	Open images	VSR	CUB
LLaVA-1.5-7B [CVPR24][26]	45.4	58.1	57.5	53.4	41.2	57.2	53.0
LLaVA-1.5-13B [CVPR24][26]	47.8	62.0	58.0	57.1	41.3	59.0	57.3
SPHINX-13B [arXiv23][24]	41.9	60.7	55.8	58.4	46.7	61.3	50.5
VisCoT-7B [NeurIPS24][44]	58.0	66.8	55.8	63.1	82.2	61.4	55.9
CogCoM [ICLR25][42]	–	–	–	71.7	–	–	–
Chain of Spot [arXiv24][30]	–	–	–	63.7	–	–	–
FAST [ICLR25][49]	–	–	–	63.8	–	–	–
Vision-R1-7B [arXiv25][16]	73.1	64.4	47.2	79.0	74.0	67.0	81.3
LMM-R1 [arXiv25][39]	69.2	61.7	52.6	80.0	76.7	40.2	64.8
R1-Onevision [arXiv25][66]	73.5	68.6	68.8	75.0	72.0	73.0	74.0
Qwen2.5-VL-7B [arXiv25][3]	72.5	64.3	50.7	81.7	78.0	57.1	52.4
Ground-R1 (Ours)	81.7	67.5	65.9	92.7	93.3	78.7	85.3
Δ (vs. Qwen2.5-VL-7B)	+9.2	+3.2	+15.2	+11.0	+15.3	+21.6	+32.9

(b)

- **Visual Grounding:** To ensure the broad coverage of multi-modal competencies, we also evaluate the visual grounding capability on RefCOCO [19], RefCOCO+ [19] and RefCOCOg [33].

Implementation Details. We conducted experiments using Qwen-2.5-VL-7B-Instruct [3]. The training was performed for 1,000 steps with a batch size of 8 and a learning rate of $1e-6$. The rollout numbers for the grounding (G_1) and answering (G_2) stages were set to 4 and 2, respectively. We used a default sampling temperature of 1 and a maximum response length of 512 tokens. All experiments were run on $8 \times$ H100 GPUs, with a total training time of approximately 12 hours.

4.2 Visual Question Answering

Evaluation Results on VisCoT. VisCoT [44] introduces the dataset focusing on scenarios where LVLMs need to concentrate on specific regions within a complete image for accurate response delivery. The dataset aggregates 12 specialized tasks structured across four reasoning tiers including document literacy (*i.e.*, DocVQA [35], TextCaps [46], TextVQA [47], DUDE [53], SROIE [17]), chart understanding (*i.e.*, InfoVQA [34]), general VQA (Flickr30k [41], Visual7W [76]), relation reasoning (*i.e.*, GQA [18], Open images [20], VSR [25]), and fine-grained VQA (*i.e.*, CUB [54]).

The evaluations on the test split of VisCoT are demonstrated in Table 2. As evidenced by the systematic evaluations, Ground-R1 demonstrates substantial performance advantages over contemporary approaches: **1)** Ground-R1 outperforms the baseline model Qwen2.5-VL-7B [3] by 9.2% on the average accuracy; **2)** Compared to the recent grounded visual reasoning approach CogCoM [42], it achieves absolute improvements of +24.2% on TextVQA [47] and +21.0% on GQA [18]; **3)** Further-

Table 3: Evaluation results on LVLM benchmarks.

Method	MME	MM-Vet	SEED	MME-RWL	RWQA	POPE
GPT-4V [37]	1926.6	67.5	53.8	–	61.4	–
GPT-4o [38]	–	69.1	72.0	–	75.4	86.9
InternVL2-8B [arXiv24] [7]	2210.3	54.2	–	–	64.4	86.9
InternVL2.5-8B [arXiv24] [6]	2344.1	62.8	–	–	70.1	90.6
Qwen2-VL-7B [arXiv24] [56]	2326.8	62.0	75.1	–	70.1	88.1
CogCoM [ICLR25] [42]	–	46.1	–	–	–	–
Chain of Spot [arXiv24] [30]	1501.1	30.8	59.7	–	–	86.4
V*[CVPR24] [60]	1128.9	27.7	41.7	–	–	82.4
FaST [ICLR25][49]	1517.4	31.0	60.1	–	–	86.4
Vision-R1-7B [arXiv25][16]	2306.2	58.3	73.0	41.0	50.2	88.7
LMM-R1 [arXiv25][39]	2210.6	64.5	74.4	35.4	52.2	86.5
R1-Onevision [arXiv25][66]	2192.2	67.5	66.5	35.1	46.5	84.9
Qwen2.5-VL-7B [arXiv25][3]	2327.0	67.1	76.5	33.8	65.9	83.6
Ground-R1 (Ours)	2360.9	69.8	76.7	46.2	66.1	89.5
Δ (vs. Qwen2.5-VL-7B)	+33.9	+2.7	+0.2	+12.4	+0.2	+5.9

more, our Ground-R1 surpasses recent R1-series works (*e.g.*, R1-Onevision [66], Vision-R1-7B [16], and LMM-R1 [39]), empirically validating that introducing evidence grounding during reasoning processes effectively enhances multi-modal task-solving capabilities.

Evaluation on LVLM Benchmarks. To ensure comprehensive evaluation, we conduct systematic benchmarking across established LVLM benchmarks including MME [10], MM-Vet [70], SEED-Bench [21], MME-RealWorld-Lite (MME-RWL) [73], and RealworldQA [62] for general capability evaluation and POPE [22] for hallucination validation.

The experimental results are presented in Table 3. Ground-R1 demonstrates significant advantages over the baseline (Qwen2.5-VL-7B [3]), existing grounded reasoning approaches [42, 50], and R1-series methods [66, 16, 39]. For instance, on the MME benchmark, Ground-R1 achieves performance improvements of 33.9 and 54.7 points compared to Qwen2.5-VL-7B and Vision-R1-7B, respectively.

4.3 Visual Grounding

We evaluate the visual grounding capabilities of Ground-R1 on RefCOCO [19], RefCOCO+ [19] and RefCOCOg [33]. We use the following prompts as follows, *i.e.*, “Locate <ref> in this image and output the bbox coordinates in JSON format.”, where <ref> refers to the specific expression.

As shown in Table 4, Ground-R1 demonstrates superior visual grounding capabilities, achieving 92.9% accuracy on RefCOCO val and surpassing most LVLMS, while narrowing the performance gap between generalist and specialist models (*e.g.*, Grounding DINO [28]). Although Ground-R1 slightly underperforms CogCoM [42] on specific benchmarks (*e.g.*, test-A of RefCOCO), this discrepancy is explainable: CogCoM leverages a specialized grounded VQA dataset [57] for additional training to enhance visual grounding, whereas our Ground-R1 maintains dual competence in both visual reasoning and grounding without requiring dedicated grounding-specific training.

4.4 Ablation Studies

To validate the superiority of our approach, we compare Ground-R1 against the following methods:

- **Ground-SFT:** This method adopts the same two-phase pipeline (*i.e.*, grounding followed by answering), but uses SFT rather than reinforcement learning for training.
- **Vanilla-SFT:** This variant removes the grounding phase in Ground-SFT and directly applies SFT training on question-answer pairs.
- **Vanilla-R1:** In contrast to Ground-R1, Vanilla-R1 omits the grounding phase and leverages reinforcement learning to train on question-answer pairs.

Table 4: Evaluation results of visual grounding on RefCOCO, RefCOCO+ and RefCOCOg.

Method	RefCOCO			RefCOCO+			RefCOCOg	
	val	test-A	test-B	val	test-A	test-B	val	test
Gemini 1.5 Pro [43]	73.2	72.9	74.6	62.5	63.9	65.0	75.2	76.2
Grounding DINO [ECCV24][28]	90.6	93.2	88.2	88.2	89.0	75.9	86.1	87.0
Shikra-7B [arXiv23] [5]	87.0	90.6	80.2	81.6	87.4	72.1	82.3	82.2
Shikra-13B [arXiv23] [5]	87.8	91.1	81.8	82.9	87.8	74.4	82.6	83.2
Qwen-VL [arXiv23] [2]	89.4	92.3	85.3	83.1	88.3	77.2	85.6	85.5
CogVLM [arXiv23] [57]	92.5	94.0	88.7	87.5	91.8	81.4	89.5	90.1
CogCoM [ICLR25] [42]	92.3	94.6	89.2	88.2	92.8	82.1	89.3	90.5
Qwen2.5-VL-7B [arXiv25][3]	90.0	92.5	85.4	84.2	89.1	76.9	87.2	87.2
InternVL2.5-8B [arXiv24][6]	90.3	94.5	85.9	85.2	91.5	78.8	86.7	87.6
Vision-R1-7B [arXiv25][16]	58.3	64.2	48.5	50.9	61.1	38.5	51.9	52.6
LMM-R1 [arXiv25][39]	87.3	91.4	83.6	79.2	87.1	72.9	84.1	84.1
R1-Onevision [arXiv25][66]	45.0	51.6	35.3	47.2	57.0	37.1	53.0	48.2
Qwen2.5-VL-7B [arXiv25][3]	90.0	92.5	85.4	84.2	89.1	76.9	87.2	87.2
Ground R1 (Ours)	92.9	93.9	88.0	86.5	90.8	78.8	90.1	90.2
Δ (vs. Qwen2.5-VL-7B)	+2.9	+1.4	+2.6	+2.3	+1.7	+1.9	+2.9	+3.0

- **Ground-R1-BBox**: This method extends Ground-R1 by incorporating ground truth bounding box supervision into the reward mechanism during the grounding phase.
- **Ground-R1-KL**: This method augments Eq (3) with a KL divergence constraints between the policy models of π_θ and $\pi_{\theta_{old}}$.

The comparison results are demonstrated in Table 5. Building upon these model variants, we seek to address four critical inquiries:

Q1: Does RL-based methodology outperform SFT-based approaches in visual reasoning?

By comparing Ground-R1 with Ground-SFT, as well as Vanilla-R1 with Vanilla-SFT, we observe that RL-based methods outperform SFT-based counterparts on most benchmarks. For example, Ground-R1 achieves an absolute improvement of 11.8% over Ground-SFT on VisCoT [44].

Q2: Does the “grounding-then-answering” paradigm outperform direct answer generation?

While “grounding-then-answering” enhances performance for RL-based methods in most cases (e.g., Ground-R1 achieves a 3.7% performance gain over Vanilla-R1 on VisCoT in Table 5), it conversely degrades performance in SFT implementations (i.e., Ground-SFT underperforms Vanilla-SFT). We posit that this limitation stems from SFT-based methods’ tendency to overfit to memorized evidence region coordinates in training data, ultimately inducing unreliable grounding localization and suboptimal predictions during testing.

Q3: What performance difference emerges when omitting bounding box rewards?

In our Ground-R1, the grounding phase is subject to only the format reward to eliminate dependency on bounding box coordinates. For systematic comparison, we further develop Ground-R1-BBox incorporating an IoU-based reward, calculated as the mean IoU between predicted and ground-truth bounding boxes. Comparative analysis (c.f. Table 5) reveals that Ground-R1 performs comparably to Ground-R1-BBox, indicating that training with RL enables accurate evidence region grounding without relying on bounding box supervision.

Q4: What is the performance difference when training with and without KL divergence constraints?

The KL divergence regularization is widely adopted in R1-related works [12, 66, 39] to prevent excessive deviation of the policy model from the reference model. However, our ablation studies in Table 5 (Ground-R1-KL vs. Ground-R1) demonstrate that removing KL constraints yields superior performance in our Ground-R1. A possible explanation is that our “grounding-then-answering” paradigm differs from the vanilla QA approach used during pre-training of the reference model; enforcing KL alignment may therefore hinder the model from fully adapting to the intermediate grounding objective and the final task reward.

Table 5: **Ablation studies of Ground-R1.** Refer to Sec 4.4 for the configuration of each model.

Method	VisCoT	MME	MM-Vet	SEED	POPE	MME-RWL	RWQA
Ground-R1	81.7	2360.9	69.8	76.7	89.5	46.2	66.1
Ground-SFT	69.9	2335.5	68.0	76.6	84.3	34.1	67.2
Vanilla-SFT	74.5	2337.0	70.1	76.7	87.6	34.2	67.1
Vanilla-R1	78.0	2338.8	53.2	75.4	88.4	35.1	66.5
Ground-R1-BBox	82.0	2356.5	70.2	75.6	88.6	46.8	66.9
Ground-R1-KL	80.0	2320.4	64.4	76.5	85.2	33.9	62.4

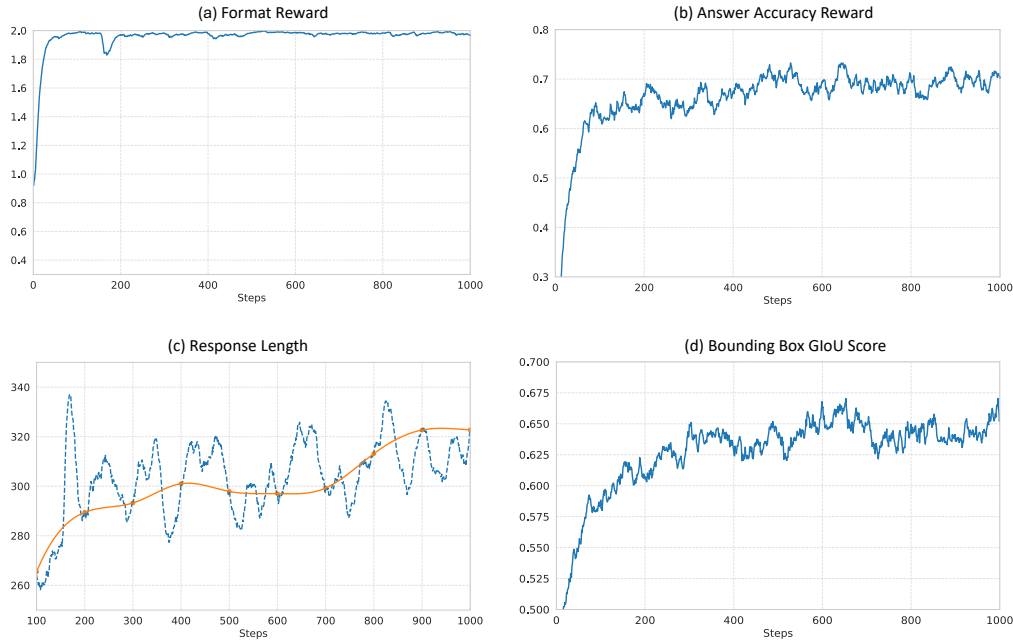


Figure 3: Visualizations of training curves of Ground-R1.

4.5 Visualizations

In Figure 3, we visualize the training curves including the format reward, answer accuracy reward, response length, and bounding box GloU scores. As shown, the format reward converges rapidly during the early training stages, while the accuracy reward stabilizes after approximately 600 steps. Additionally, the response length gradually increases with training steps, indicating the emergence of longer reasoning chains. As shown in Figure 3(d), the accuracy of the evidence regions generated by Ground-R1 steadily improves throughout training, reaching approximately 67.5%, despite the absence of bounding box supervision in the RL training process.

5 Conclusion

We present Ground-R1, an RL framework for grounded visual reasoning that removes the dependency on costly evidence annotations. By decoupling the reasoning process into grounding and answering phases, Ground-R1 effectively aligns visual evidence with textual responses under reward-driven supervision. Our method demonstrates strong empirical performance across diverse benchmarks, surpassing both supervised fine-tuning and prior grounded reasoning approaches. Moreover, Ground-R1 exhibits emergent behaviors such as uncertainty awareness, spatial perception, and iterative refinement, offering a scalable and interpretable alternative for advancing trustworthy LVLM reasoning.

References

- [1] Anthropic. Claude 3.5 sonnet, 2024.
- [2] Jinze Bai, Shuai Bai, Shusheng Yang, Shijie Wang, Sinan Tan, Peng Wang, Junyang Lin, Chang Zhou, and Jingren Zhou. Qwen-vl: A frontier large vision-language model with versatile abilities. *arXiv preprint arXiv:2308.12966*, 2023.
- [3] Shuai Bai, Keqin Chen, Xuejing Liu, Jialin Wang, Wenbin Ge, Sibao Song, Kai Dang, Peng Wang, Shijie Wang, Jun Tang, et al. Qwen2. 5-vl technical report. *arXiv preprint arXiv:2502.13923*, 2025.
- [4] Maciej Besta, Nils Blach, Ales Kubicek, Robert Gerstenberger, Michal Podstawski, Lukas Gianinazzi, Joanna Gajda, Tomasz Lehmann, Hubert Niewiadomski, Piotr Nyczyk, et al. Graph of thoughts: Solving elaborate problems with large language models. In *Proceedings of the AAAI Conference on Artificial Intelligence*, volume 38, pages 17682–17690, 2024.
- [5] Keqin Chen, Zhao Zhang, Weili Zeng, Richong Zhang, Feng Zhu, and Rui Zhao. Shikra: Unleashing multimodal llm’s referential dialogue magic. *arXiv preprint arXiv:2306.15195*, 2023.
- [6] Zhe Chen, Weiyun Wang, Yue Cao, Yangzhou Liu, Zhangwei Gao, Erfei Cui, Jinguo Zhu, Shenglong Ye, Hao Tian, Zhaoyang Liu, et al. Expanding performance boundaries of open-source multimodal models with model, data, and test-time scaling. *arXiv preprint arXiv:2412.05271*, 2024.
- [7] Zhe Chen, Weiyun Wang, Hao Tian, Shenglong Ye, Zhangwei Gao, Erfei Cui, Wenwen Tong, Kongzhi Hu, Jiapeng Luo, Zheng Ma, et al. How far are we to gpt-4v? closing the gap to commercial multimodal models with open-source suites. *arXiv preprint arXiv:2404.16821*, 2024.
- [8] Zhenfang Chen, Qinhong Zhou, Yikang Shen, Yining Hong, Hao Zhang, and Chuang Gan. See, think, confirm: Interactive prompting between vision and language models for knowledge-based visual reasoning. *arXiv preprint arXiv:2301.05226*, 2023.
- [9] Yuhao Dong, Zuyan Liu, Hai-Long Sun, Jingkan Yang, Winston Hu, Yongming Rao, and Ziwei Liu. Insight-v: Exploring long-chain visual reasoning with multimodal large language models. *arXiv preprint arXiv:2411.14432*, 2024.
- [10] Chaoyou Fu, Peixian Chen, Yunhang Shen, Yulei Qin, Mengdan Zhang, Xu Lin, Jinrui Yang, Xiawu Zheng, Ke Li, Xing Sun, et al. Mme: A comprehensive evaluation benchmark for multimodal large language models, 2024. URL <https://arxiv.org/abs/2306.13394>, 2.
- [11] Xingyu Fu, Minqian Liu, Zhengyuan Yang, John Corring, Yijuan Lu, Jianwei Yang, Dan Roth, Dinei Florencio, and Cha Zhang. Refocus: Visual editing as a chain of thought for structured image understanding. *arXiv preprint arXiv:2501.05452*, 2025.
- [12] Daya Guo, Dejian Yang, Haowei Zhang, Junxiao Song, Ruoyu Zhang, Runxin Xu, Qihao Zhu, Shirong Ma, Peiyi Wang, Xiao Bi, et al. Deepseek-r1: Incentivizing reasoning capability in llms via reinforcement learning. *arXiv preprint arXiv:2501.12948*, 2025.
- [13] Shashank Gupta, Vaishnavi Shrivastava, Ameet Deshpande, Ashwin Kalyan, Peter Clark, Ashish Sabharwal, and Tushar Khot. Bias runs deep: Implicit reasoning biases in persona-assigned llms. *arXiv preprint arXiv:2311.04892*, 2023.
- [14] Yushi Hu, Weijia Shi, Xingyu Fu, Dan Roth, Mari Ostendorf, Luke Zettlemoyer, Noah A Smith, and Ranjay Krishna. Visual sketchpad: Sketching as a visual chain of thought for multimodal language models. *arXiv preprint arXiv:2406.09403*, 2024.
- [15] Jie Huang and Kevin Chen-Chuan Chang. Towards reasoning in large language models: A survey. In *Findings of the Association for Computational Linguistics: ACL 2023*, pages 1049–1065, 2023.

- [16] Wenxuan Huang, Bohan Jia, Zijie Zhai, Shaosheng Cao, Zheyu Ye, Fei Zhao, Zhe Xu, Yao Hu, and Shaohui Lin. Vision-r1: Incentivizing reasoning capability in multimodal large language models. *arXiv preprint arXiv:2503.06749*, 2025.
- [17] Zheng Huang, Kai Chen, Jianhua He, Xiang Bai, Dimosthenis Karatzas, Shijian Lu, and CV Jawahar. Icdar2019 competition on scanned receipt ocr and information extraction. In *2019 International Conference on Document Analysis and Recognition (ICDAR)*, pages 1516–1520. IEEE, 2019.
- [18] Drew A Hudson and Christopher D Manning. Gqa: A new dataset for real-world visual reasoning and compositional question answering. In *Proceedings of the IEEE/CVF conference on computer vision and pattern recognition*, pages 6700–6709, 2019.
- [19] Sahar Kazemzadeh, Vicente Ordonez, Mark Matten, and Tamara Berg. Referitgame: Referring to objects in photographs of natural scenes. In *Proceedings of the 2014 conference on empirical methods in natural language processing (EMNLP)*, pages 787–798, 2014.
- [20] Alina Kuznetsova, Hassan Rom, Neil Alldrin, Jasper Uijlings, Ivan Krasin, Jordi Pont-Tuset, Shahab Kamali, Stefan Popov, Matteo Mallocci, Alexander Kolesnikov, et al. The open images dataset v4: Unified image classification, object detection, and visual relationship detection at scale. *International journal of computer vision*, 128(7):1956–1981, 2020.
- [21] Bohao Li, Rui Wang, Guangzhi Wang, Yuying Ge, Yixiao Ge, and Ying Shan. Seed-bench: Benchmarking multimodal llms with generative comprehension. *arXiv preprint arXiv:2307.16125*, 2023.
- [22] Yifan Li, Yifan Du, Kun Zhou, Jinpeng Wang, Wayne Xin Zhao, and Ji-Rong Wen. Evaluating object hallucination in large vision-language models. *arXiv preprint arXiv:2305.10355*, 2023.
- [23] Zejun Li, Ruipu Luo, Jiwen Zhang, Minghui Qiu, Xuanjing Huang, and Zhongyu Wei. Vocot: Unleashing visually grounded multi-step reasoning in large multi-modal models. *arXiv preprint arXiv:2405.16919*, 2024.
- [24] Ziyi Lin, Chris Liu, Renrui Zhang, Peng Gao, Longtian Qiu, Han Xiao, Han Qiu, Chen Lin, Wenqi Shao, Keqin Chen, et al. Sphinx: The joint mixing of weights, tasks, and visual embeddings for multi-modal large language models. *arXiv preprint arXiv:2311.07575*, 2023.
- [25] Fangyu Liu, Guy Emerson, and Nigel Collier. Visual spatial reasoning. *Transactions of the Association for Computational Linguistics*, 11:635–651, 2023.
- [26] Haotian Liu, Chunyuan Li, Yuheng Li, and Yong Jae Lee. Improved baselines with visual instruction tuning. In *Proceedings of the IEEE/CVF Conference on Computer Vision and Pattern Recognition*, pages 26296–26306, 2024.
- [27] Shilong Liu, Hao Cheng, Haotian Liu, Hao Zhang, Feng Li, Tianhe Ren, Xueyan Zou, Jianwei Yang, Hang Su, Jun Zhu, et al. Llava-plus: Learning to use tools for creating multimodal agents. *arXiv preprint arXiv:2311.05437*, 2023.
- [28] Shilong Liu, Zhaoyang Zeng, Tianhe Ren, Feng Li, Hao Zhang, Jie Yang, Qing Jiang, Chunyuan Li, Jianwei Yang, Hang Su, et al. Grounding dino: Marrying dino with grounded pre-training for open-set object detection. In *European Conference on Computer Vision*, pages 38–55. Springer, 2024.
- [29] Ziyu Liu, Zeyi Sun, Yuhang Zang, Xiaoyi Dong, Yuhang Cao, Haodong Duan, Dahua Lin, and Jiaqi Wang. Visual-rft: Visual reinforcement fine-tuning. *arXiv preprint arXiv:2503.01785*, 2025.
- [30] Zuyan Liu, Yuhao Dong, Yongming Rao, Jie Zhou, and Jiwen Lu. Chain-of-spot: Interactive reasoning improves large vision-language models. *arXiv preprint arXiv:2403.12966*, 2024.
- [31] Trung Quoc Luong, Xinbo Zhang, Zhanming Jie, Peng Sun, Xiaoran Jin, and Hang Li. Reft: Reasoning with reinforced fine-tuning. *arXiv preprint arXiv:2401.08967*, 3, 2024.

- [32] Zixian Ma, Jianguo Zhang, Zhiwei Liu, Jieyu Zhang, Juntao Tan, Manli Shu, Juan Carlos Niebles, Shelby Heinecke, Huan Wang, Caiming Xiong, et al. Taco: Learning multi-modal action models with synthetic chains-of-thought-and-action. *arXiv preprint arXiv:2412.05479*, 2024.
- [33] Junhua Mao, Jonathan Huang, Alexander Toshev, Oana Camburu, Alan L Yuille, and Kevin Murphy. Generation and comprehension of unambiguous object descriptions. In *Proceedings of the IEEE conference on computer vision and pattern recognition*, pages 11–20, 2016.
- [34] Minesh Mathew, Viraj Bagal, Rubèn Tito, Dimosthenis Karatzas, Ernest Valveny, and CV Jawahar. Infographicvqa. In *Proceedings of the IEEE/CVF Winter Conference on Applications of Computer Vision*, pages 1697–1706, 2022.
- [35] Minesh Mathew, Dimosthenis Karatzas, and CV Jawahar. Docvqa: A dataset for vqa on document images. In *Proceedings of the IEEE/CVF winter conference on applications of computer vision*, pages 2200–2209, 2021.
- [36] Fanqing Meng, Lingxiao Du, Zongkai Liu, Zhixiang Zhou, Quanfeng Lu, Daocheng Fu, Tiancheng Han, Botian Shi, Wenhai Wang, Junjun He, et al. Mm-eureka: Exploring the frontiers of multimodal reasoning with rule-based reinforcement learning. *arXiv preprint arXiv:2503.07365*, 2025.
- [37] OpenAI. Gpt-4v(ision) system card. <https://api.semanticscholar.org/CorpusID:263218031>, 2023.
- [38] OpenAI. Hello gpt-4o. *OpenAI Blog*, 2024.
- [39] Yingzhe Peng, Gongrui Zhang, Miaosen Zhang, Zhiyuan You, Jie Liu, Qipeng Zhu, Kai Yang, Xingzhong Xu, Xin Geng, and Xu Yang. Lmm-r1: Empowering 3b lms with strong reasoning abilities through two-stage rule-based rl. *arXiv preprint arXiv:2503.07536*, 2025.
- [40] Zhiliang Peng, Wenhui Wang, Li Dong, Yaru Hao, Shaohan Huang, Shuming Ma, and Furu Wei. Kosmos-2: Grounding multimodal large language models to the world. *arXiv preprint arXiv:2306.14824*, 2023.
- [41] Bryan A Plummer, Liwei Wang, Chris M Cervantes, Juan C Caicedo, Julia Hockenmaier, and Svetlana Lazebnik. Flickr30k entities: Collecting region-to-phrase correspondences for richer image-to-sentence models. In *Proceedings of the IEEE international conference on computer vision*, pages 2641–2649, 2015.
- [42] Ji Qi, Ming Ding, Weihang Wang, Yushi Bai, Qingsong Lv, Wenyi Hong, Bin Xu, Lei Hou, Juanzi Li, Yuxiao Dong, et al. Cogcom: Train large vision-language models diving into details through chain of manipulations. *arXiv preprint arXiv:2402.04236*, 2024.
- [43] Machel Reid, Nikolay Savinov, Denis Teplyashin, Dmitry Lepikhin, Timothy Lillicrap, Jean-baptiste Alayrac, Radu Soricut, Angeliki Lazaridou, Orhan Firat, Julian Schrittwieser, et al. Gemini 1.5: Unlocking multimodal understanding across millions of tokens of context. *arXiv preprint arXiv:2403.05530*, 2024.
- [44] Hao Shao, Shengju Qian, Han Xiao, Guanglu Song, Zhuofan Zong, Letian Wang, Yu Liu, and Hongsheng Li. Visual cot: Advancing multi-modal language models with a comprehensive dataset and benchmark for chain-of-thought reasoning. *Advances in Neural Information Processing Systems*, 37:8612–8642, 2024.
- [45] Zhihong Shao, Peiyi Wang, Qihao Zhu, Runxin Xu, Junxiao Song, Xiao Bi, Haowei Zhang, Mingchuan Zhang, YK Li, Y Wu, et al. Deepseekmath: Pushing the limits of mathematical reasoning in open language models. *arXiv preprint arXiv:2402.03300*, 2024.
- [46] Oleksii Sidorov, Ronghang Hu, Marcus Rohrbach, and Amanpreet Singh. Textcaps: a dataset for image captioning with reading comprehension. In *Computer Vision—ECCV 2020: 16th European Conference, Glasgow, UK, August 23–28, 2020, Proceedings, Part II 16*, pages 742–758. Springer, 2020.

- [47] Amanpreet Singh, Vivek Natarajan, Meet Shah, Yu Jiang, Xinlei Chen, Dhruv Batra, Devi Parikh, and Marcus Rohrbach. Towards vqa models that can read. In *Proceedings of the IEEE/CVF conference on computer vision and pattern recognition*, pages 8317–8326, 2019.
- [48] Zhaochen Su, Linjie Li, Mingyang Song, Yunzhuo Hao, Zhengyuan Yang, Jun Zhang, Guanjie Chen, Jiawei Gu, Juntao Li, Xiaoye Qu, and Yu Cheng. Openthinking: Learning to think with images via visual tool reinforcement learning. *arXiv preprint arXiv:2505.08617*, 2025.
- [49] Guangyan Sun, Mingyu Jin, Zhenting Wang, Cheng-Long Wang, Siqi Ma, Qifan Wang, Tong Geng, Ying Nian Wu, Yongfeng Zhang, and Dongfang Liu. Visual agents as fast and slow thinkers. *arXiv preprint arXiv:2408.08862*, 2024.
- [50] Guangyan Sun, Mingyu Jin, Zhenting Wang, Cheng-Long Wang, Siqi Ma, Qifan Wang, Tong Geng, Ying Nian Wu, Yongfeng Zhang, and Dongfang Liu. Visual agents as fast and slow thinkers. In *The Thirteenth International Conference on Learning Representations*, 2025.
- [51] Huajie Tan, Yuheng Ji, Xiaoshuai Hao, Minglan Lin, Pengwei Wang, Zhongyuan Wang, and Shanghang Zhang. Reason-rft: Reinforcement fine-tuning for visual reasoning. *arXiv preprint arXiv:2503.20752*, 2025.
- [52] Omkar Thawakar, Dinura Dissanayake, Ketan More, Ritesh Thawkar, Ahmed Heakl, Noor Ahsan, Yuhao Li, Mohammed Zumri, Jean Lahoud, Rao Muhammad Anwer, et al. Llamav-o1: Rethinking step-by-step visual reasoning in llms. *arXiv preprint arXiv:2501.06186*, 2025.
- [53] Jordy Van Landeghem, Rubèn Tito, Łukasz Borchmann, Michał Pietruszka, Paweł Joziak, Rafał Powalski, Dawid Jurkiewicz, Mickaël Coustaty, Bertrand Anckaert, Ernest Valveny, et al. Document understanding dataset and evaluation (dude). In *Proceedings of the IEEE/CVF International Conference on Computer Vision*, pages 19528–19540, 2023.
- [54] Catherine Wah, Steve Branson, Peter Welinder, Pietro Perona, and Serge Belongie. The caltech-ucsd birds-200-2011 dataset. 2011.
- [55] Lei Wang, Yi Hu, Jiabang He, Xing Xu, Ning Liu, Hui Liu, and Heng Tao Shen. T-sciq: Teaching multimodal chain-of-thought reasoning via large language model signals for science question answering. In *Proceedings of the AAAI Conference on Artificial Intelligence*, volume 38, pages 19162–19170, 2024.
- [56] Peng Wang, Shuai Bai, Sinan Tan, Shijie Wang, Zhihao Fan, Jinze Bai, Keqin Chen, Xuejing Liu, Jialin Wang, Wenbin Ge, et al. Qwen2-vl: Enhancing vision-language model’s perception of the world at any resolution. *arXiv preprint arXiv:2409.12191*, 2024.
- [57] Weihang Wang, Qingsong Lv, Wenmeng Yu, Wenyi Hong, Ji Qi, Yan Wang, Junhui Ji, Zhuoyi Yang, Lei Zhao, Song XiXuan, et al. Cogvlm: Visual expert for pretrained language models. *Advances in Neural Information Processing Systems*, 37:121475–121499, 2024.
- [58] Yaoting Wang, Shengqiong Wu, Yuecheng Zhang, William Wang, Ziwei Liu, Jiebo Luo, and Hao Fei. Multimodal chain-of-thought reasoning: A comprehensive survey. *arXiv preprint arXiv:2503.12605*, 2025.
- [59] Jason Wei, Xuezhi Wang, Dale Schuurmans, Maarten Bosma, Fei Xia, Ed Chi, Quoc V Le, Denny Zhou, et al. Chain-of-thought prompting elicits reasoning in large language models. *Advances in neural information processing systems*, 35:24824–24837, 2022.
- [60] Penghao Wu and Saining Xie. V?: Guided visual search as a core mechanism in multimodal llms. In *Proceedings of the IEEE/CVF Conference on Computer Vision and Pattern Recognition*, pages 13084–13094, 2024.
- [61] Qiong Wu, Xiangcong Yang, Yiyi Zhou, Chenxin Fang, Baiyang Song, Xiaoshuai Sun, and Rongrong Ji. Grounded chain-of-thought for multimodal large language models. *arXiv preprint arXiv:2503.12799*, 2025.
- [62] xAI. Grok-1.5v, 2024. Accessed: 2024-05-16.

- [63] Fengli Xu, Qianyue Hao, Zefang Zong, Jingwei Wang, Yunke Zhang, Jingyi Wang, Xiaochong Lan, Jiahui Gong, Tianjian Ouyang, Fanjin Meng, et al. Towards large reasoning models: A survey of reinforced reasoning with large language models. *arXiv preprint arXiv:2501.09686*, 2025.
- [64] Guowei Xu, Peng Jin, Li Hao, Yibing Song, Lichao Sun, and Li Yuan. Llava-o1: Let vision language models reason step-by-step. *arXiv preprint arXiv:2411.10440*, 2024.
- [65] Wenda Xu, Guanglei Zhu, Xuandong Zhao, Liangming Pan, Lei Li, and William Yang Wang. Pride and prejudice: Llm amplifies self-bias in self-refinement. *arXiv preprint arXiv:2402.11436*, 2024.
- [66] Yi Yang, Xiaoxuan He, Hongkun Pan, Xiyan Jiang, Yan Deng, Xingtao Yang, Haoyu Lu, Dacheng Yin, Fengyun Rao, Minfeng Zhu, et al. R1-onevision: Advancing generalized multimodal reasoning through cross-modal formalization. *arXiv preprint arXiv:2503.10615*, 2025.
- [67] Huanjin Yao, Jiaying Huang, Wenhao Wu, Jingyi Zhang, Yibo Wang, Shunyu Liu, Yingjie Wang, Yuxin Song, Haocheng Feng, Li Shen, et al. Mulberry: Empowering mllm with o1-like reasoning and reflection via collective monte carlo tree search. *arXiv preprint arXiv:2412.18319*, 2024.
- [68] Shunyu Yao, Dian Yu, Jeffrey Zhao, Izhak Shafran, Tom Griffiths, Yuan Cao, and Karthik Narasimhan. Tree of thoughts: Deliberate problem solving with large language models. *Advances in neural information processing systems*, 36:11809–11822, 2023.
- [69] En Yu, Kangheng Lin, Liang Zhao, Jisheng Yin, Yana Wei, Yuang Peng, Haoran Wei, Jianjian Sun, Chunrui Han, Zheng Ge, et al. Perception-r1: Pioneering perception policy with reinforcement learning. *arXiv preprint arXiv:2504.07954*, 2025.
- [70] Weihao Yu, Zhengyuan Yang, Linjie Li, Jianfeng Wang, Kevin Lin, Zicheng Liu, Xinchao Wang, and Lijuan Wang. Mm-vet: Evaluating large multimodal models for integrated capabilities. *arXiv preprint arXiv:2308.02490*, 2023.
- [71] Jiarui Zhang, Mahyar Khayatkhoei, Prateek Chhikara, and Filip Ilievski. Mllms know where to look: Training-free perception of small visual details with multimodal llms. *arXiv preprint arXiv:2502.17422*, 2025.
- [72] Shilong Zhang, Peize Sun, Shoufa Chen, Minn Xiao, Wenqi Shao, Wenwei Zhang, Yu Liu, Kai Chen, and Ping Luo. Gpt4roi: Instruction tuning large language model on regionof-interest, 2024. In URL <https://openreview.net/forum>.
- [73] Yi-Fan Zhang, Huanyu Zhang, Haochen Tian, Chaoyou Fu, Shuangqing Zhang, Junfei Wu, Feng Li, Kun Wang, Qingsong Wen, Zhang Zhang, et al. Mme-realworld: Could your multimodal llm challenge high-resolution real-world scenarios that are difficult for humans? *arXiv preprint arXiv:2408.13257*, 2024.
- [74] Zhuosheng Zhang, Aston Zhang, Mu Li, Hai Zhao, George Karypis, and Alex Smola. Multimodal chain-of-thought reasoning in language models. *arXiv preprint arXiv:2302.00923*, 2023.
- [75] Hanzhang Zhou, Zijian Feng, Zixiao Zhu, Junlang Qian, and Kezhi Mao. Unibias: Unveiling and mitigating llm bias through internal attention and ffn manipulation. *arXiv preprint arXiv:2405.20612*, 2024.
- [76] Yuke Zhu, Oliver Groth, Michael Bernstein, and Li Fei-Fei. Visual7w: Grounded question answering in images. In *Proceedings of the IEEE conference on computer vision and pattern recognition*, pages 4995–5004, 2016.

A Limitations and Broader Impacts

Limitations. While Ground-R1 demonstrates promising results, several limitations warrant discussion. First, the grounding-answering pipeline introduces additional inference overhead compared to end-to-end methods, potentially affecting deployment efficiency. Secondly, due to the lack of explicit supervision for grounding, the generated evidence regions may be imprecise or suboptimal, especially in complex scenes. We leave the exploration of more flexible and efficient grounding strategies for future work.

Broader Impacts. The positive social impact of this work is that it enhances LVLMs with grounded visual reasoning capabilities, making existing LVLMs more “smart” and “logical”, and enabling them to provide more accurate answers to users’ questions. The potential negative social impact of this work is that it may raise privacy concerns among users, especially when visual reasoning needs to be performed on private images uploaded by users. A possible solution is to clearly inform users that the model will perform grounded visual reasoning based on the uploaded images, and to provide them with the option to opt out of visual reasoning.

B More Ablation Studies

Ablations of hyper-parameters. We conduct the ablation studies with different grounding rollout numbers G_1 and answering rollout numbers G_2 . The results in Table 6 demonstrate that the optimum performance is achieved when setting $G_1 = 4$ and $G_2 = 2$.

Table 6: Ablations of hyper-parameters.

Method	VisCoT	MME	MM-Vet	SEED	POPE	MME-RWL	RWQA
$G_1 = 1, G_2 = 8$	80.4	2345.0	68.3	76.3	89.3	45.1	64.4
$G_1 = 2, G_2 = 4$	80.0	2321.3	66.3	76.0	89.7	44.2	67.1
$G_1 = 4, G_2 = 2$	81.7	2360.9	69.8	76.7	89.5	46.2	66.1
$G_1 = 8, G_2 = 1$	80.6	2349.0	66.0	76.3	89.5	42.9	60.3

Visualizations. The reasoning trajectories of Ground-R1 are visualized in Figure 4 - Figure 8. Specifically, the cases in Figure 4, Figure 5, Figure 6 require three zoom-in operations to obtain the final answer while the cases in Figure 7 require one zoom-in operation. In particular, the cases in Figure 8 do not require zoom-in operation and directly answer the questions.

Number distribution of zoom-in operations. We count the number of zoom-in operations N used during inference (*i.e.*, the number of occurrences of `<box>` and `</box>` in the reasoning trace). The statistics in Table 7 show that most questions (78%) can be answered with two zoom-in steps, while a small portion (5%) can be solved directly without any zoom-in operations ($N = 0$).

Table 7: Distribution of zoom-in operation numbers.

N	0	1	2	≥ 3
Percentage	5%	12%	78%	5%

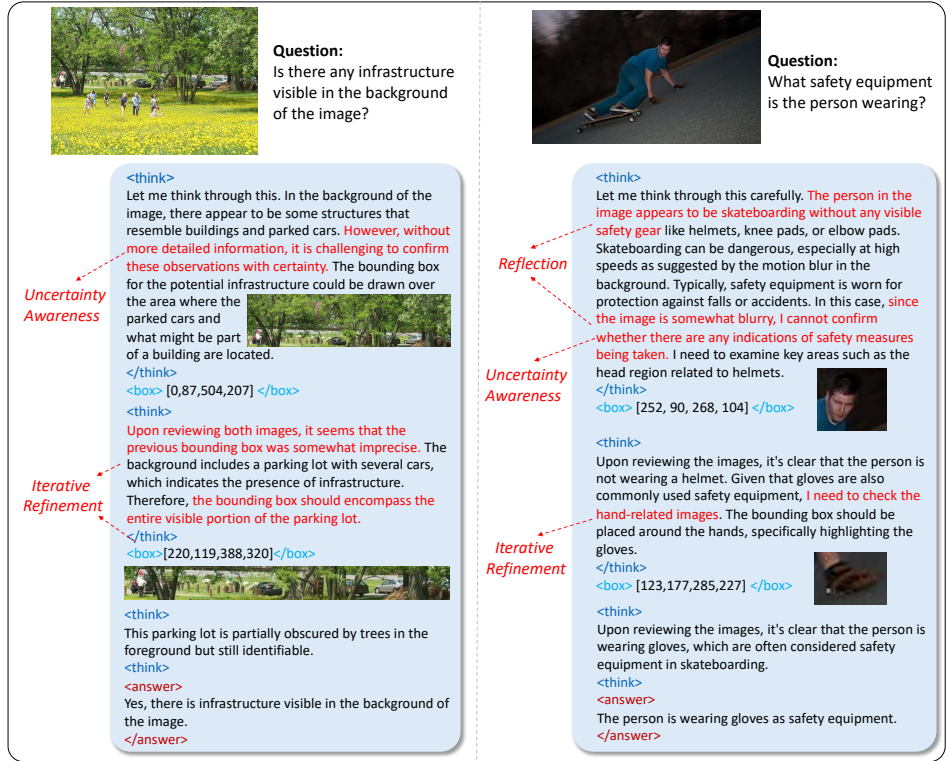


Figure 4: Reasoning trajectories of Ground-R1.

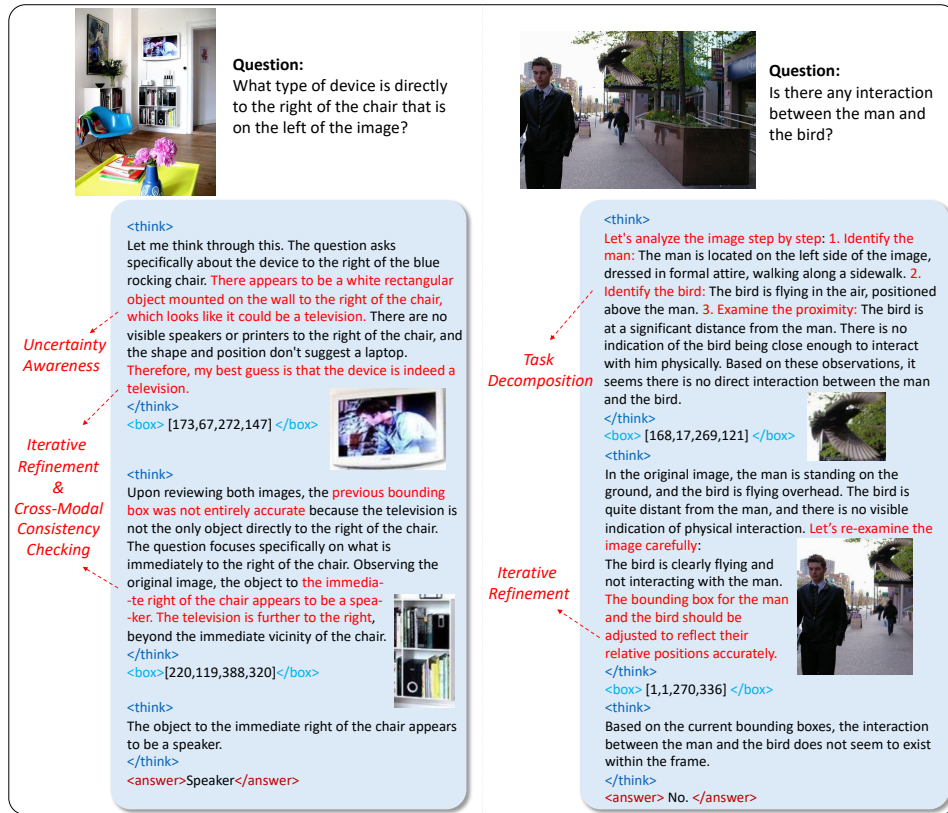


Figure 5: Reasoning trajectories of Ground-R1.

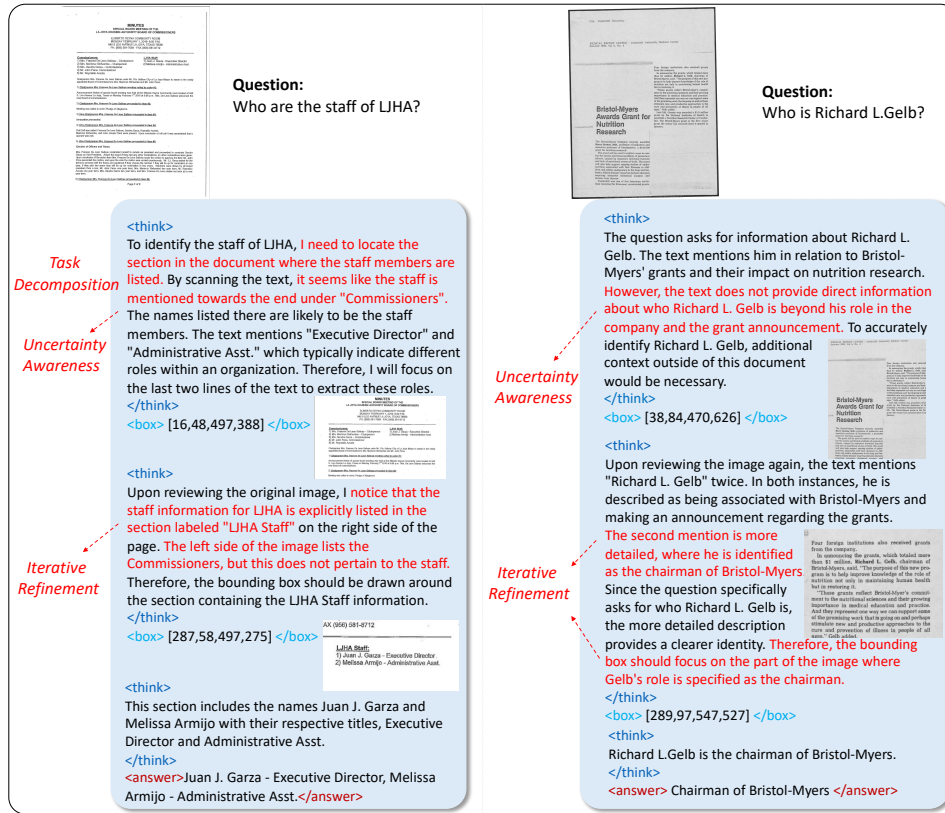


Figure 6: Reasoning trajectories of Ground-R1.

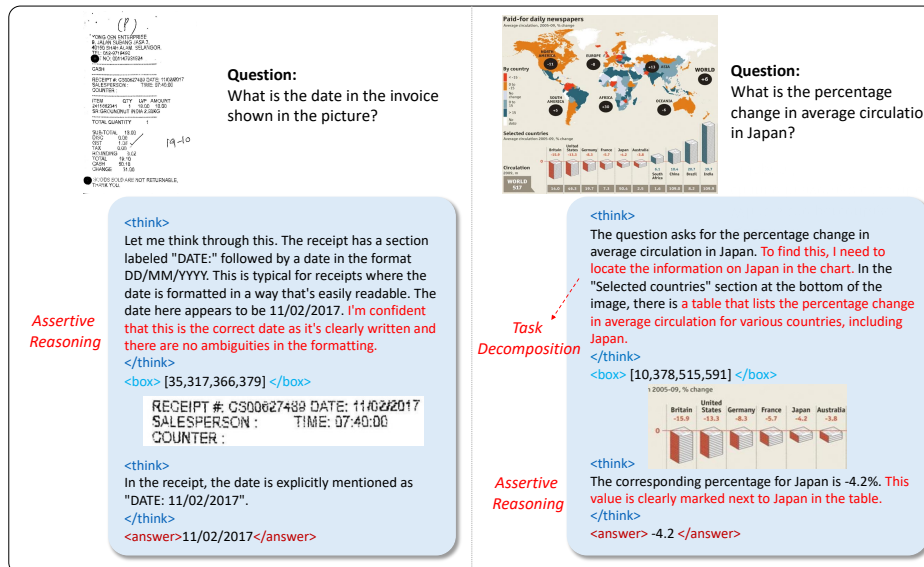


Figure 7: Reasoning trajectories of Ground-R1.



Question:
What brand of watch is this?

Assertive Reasoning & Self-Examination

<think>
Let me think about this. The watch is clearly visible inside an open box, and there is text on the box and the watch itself that reads "TUDOR." This is enough to identify the brand. The packaging also has "TUDOR" printed multiple times, which reinforces the brand identification. Therefore, based on these visual cues, the brand of the watch is TUDOR.
</think>
<answer>TUDOR</answer>



Question:
What color is the rock mentioned?

Assertive Reasoning

<think>
The question asks about the color of the rock mentioned. The word "WHITE" directly describes the color of the rock, which is white. There is no ambiguity here, so we can confidently identify the color.
</think>
<answer>White</answer>



Question:
What is this a gateway to?

Assertive Reasoning

<think>
This is a postcard-like image advertising the Sun Dial Motel in Williams, Arizona. The text explicitly states "Gateway to Grand Canyon" at the bottom left corner.
</think>
<answer>Grand Canyon</answer>



Question:
Where is the boat resting?

Assertive Reasoning

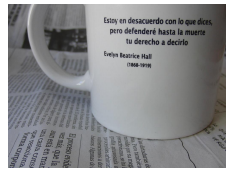
<think>
In the image, the boat is positioned prominently in the center with a rock formation underneath it. The boat is resting on a cluster of large rocks that appear to be supporting its hull. The rocks are clearly visible and serve as the resting place for the boat, which is supported by their solid foundation.
</think>
<answer>
The boat is resting on a group of rocks.
</answer>



Question:
What are headed the same way?

Assertive Reasoning

<think>
Let me think through this. The question asks what vehicles are headed the same way. By looking at the image, we can see a group of cars on the left side of the road, all facing forward towards the direction of the Ferry Building. There doesn't appear to be any significant traffic flow in the opposite direction.
</think>
<answer>The cars are headed the same way.</answer>



Question:
Whose quote is displayed on the white mug?

Assertive Reasoning

<think>
Let me think about this. The quote on the mug reads "Estoy en desacuerdo con lo que dices, pero defenderé hasta la muerte tu derecho a decirlo." The attribution below the quote mentions "Evelyn Beatrice Hall (1868-1919)." Given that Evelyn Beatrice Hall is the person mentioned, it is reasonable to conclude that her quote is displayed on the mug.
</think>
<answer>Evelyn Beatrice Hall</answer>

Figure 8: Reasoning trajectories of Ground-R1.